ARL-TR-9627 ● JAN 2023

DEVCOM ARMY RESEARCH LABORATORY

Stepped-Frequency Distributed Radar for Through-the-Wall Sensing: Resolution of Moving Targets by Orthogonal Antenna Pairs

by Gregory J Mazzaro and David M McNamara

Approved for public release: distribution unlimited.

NOTICES

Disclaimers

The findings in this report are not to be construed as an official Department of the Army position unless so designated by other authorized documents.

Citation of manufacturer's or trade names does not constitute an official endorsement or approval of the use thereof.

Destroy this report when it is no longer needed. Do not return it to the originator.

ARL-TR-9627 ● JAN 2023

Stepped-Frequency Distributed Radar for Through-the-Wall Sensing: Resolution of Moving Targets by Orthogonal Antenna Pairs

Gregory J Mazzaro
The Citadel, The Military College of South Carolina

David M McNamara
DEVCOM Army Research Laboratory

Approved for public release: distribution unlimited.

REPORT DOCUMENTATION PAGE

Form Approved
OMB No. 0704-0188

Public reporting burden for this collection of information is estimated to average 1 hour per response, including the time for reviewing instructions, searching existing data sources, gathering and maintaining the data needed, and completing and reviewing the collection information. Send comments regarding this burden estimate or any other aspect of this collection of information, including suggestions for reducing the burden, to Department of Defense, Washington Headquarters Services, Directorate for Information Operations and Reports (0704-0188), 1215 Jefferson Davis Highway, Suite 1204, Arlington, VA 22202-4302. Respondents should be aware that notwithstanding any other provision of law, no person shall be subject to any penalty for failing to comply with a collection of information if it does not display a currently valid OMB control number.
PLEASE DO NOT RETURN YOUR FORM TO THE ABOVE ADDRESS.

1. REPORT DATE *(DD-MM-YYYY)*	2. REPORT TYPE	3. DATES COVERED (From - To)
January 2023	Technical Report	15 June–15 August 2022

4. TITLE AND SUBTITLE
Stepped-Frequency Distributed Radar for Through-the-Wall Sensing: Resolution of Moving Targets by Orthogonal Antenna Pairs

5a. CONTRACT NUMBER

5b. GRANT NUMBER

5c. PROGRAM ELEMENT NUMBER

6. AUTHOR(S)
Gregory J Mazzaro and David M McNamara

5d. PROJECT NUMBER

5e. TASK NUMBER

5f. WORK UNIT NUMBER

7. PERFORMING ORGANIZATION NAME(S) AND ADDRESS(ES)
DEVCOM Army Research Laboratory
ATTN: FCDD-RLA-LC
Adelphi, MD 20783-1138

8. PERFORMING ORGANIZATION REPORT NUMBER
ARL-TR-9627

9. SPONSORING/MONITORING AGENCY NAME(S) AND ADDRESS(ES)

10. SPONSOR/MONITOR'S ACRONYM(S)

11. SPONSOR/MONITOR'S REPORT NUMBER(S)

12. DISTRIBUTION/AVAILABILITY STATEMENT
Approved for public release: distribution unlimited.

13. SUPPLEMENTARY NOTES
ORCID ID: Gregory Mazzaro, 0000-0001-5814-7425

14. ABSTRACT
The authors studied distributed radar for through-the-wall sensing. The intended application is detection and identification of personnel and weaponry located inside of a building from outside of that building. The radar architecture used for this study is similar to one recently implemented by US Army Combat Capabilities Development Command Army Research Laboratory researchers for concealed-target detection. Experiments were conducted at the Adelphi Laboratory Center in Building 507 using the low-metal plywood structure recently used for synthetic-aperture and harmonic-radar tests.

15. SUBJECT TERMS
Weapons Sciences, radar, distributed, through-the-wall, sensing, plywood, range profile

16. SECURITY CLASSIFICATION OF:			17. LIMITATION OF ABSTRACT	18. NUMBER OF PAGES	19a. NAME OF RESPONSIBLE PERSON
a. REPORT	b. ABSTRACT	c. THIS PAGE			Gregory Mazzaro
Unclassified	Unclassified	Unclassified	UU	28	19b. TELEPHONE NUMBER (Include area code) gregory.j.mazzaro.ctr@army.mil

Standard Form 298 (Rev. 8/98)
Prescribed by ANSI Std. Z39.18

Contents

List of Figures

1. Introduction

The authors are studying the application of distributed radar to through-the-wall sensing. The intended operational scenario for this technology is detection and identification of personnel and weaponry located inside of a building from a (safe) remote standoff distance outside of that building.[1,2] The radar architecture and signal-processing algorithms used for this study are similar to the designs implemented by the US Army Combat Capabilities Development Command (DEVCOM) Army Research Laboratory (ARL) for buried- and concealed-surface-target detection[3,4]; the current radar transmits and receives higher frequencies.

For this study, experiments were conducted at ARL's Adelphi Laboratory Center (ALC) in Building 507 (the "sandbox" area) using the indoor low-metal two-story plywood structure. The controlled environment used to test the distributed radar is the same as the low-metal environment used to test ARL's harmonic radar against electronic targets.[5]

2. Experiment: Hardware and Test Environment

The radar transceiver was developed by Alion Science & Technology, recently acquired by Huntington Ingalls Industries (HII). The waveform generation-and-capture core of the radar is the Zynq UltraScale+ radio-frequency system-on-a-chip (RFSoC) manufactured by Xilinx. The RFSoC evaluation board, packaged by Alion/HII and controllable by a graphical user interface (GUI) over Ethernet, is shown in Fig. 1a. The GUI is labeled "Non-Linear Radar" because the hardware and firmware were originally developed with the ability to transmit a (lower) band of frequencies while receiving a harmonic (higher) band of frequencies.[6]

The RFSoC generates a constant-amplitude stepped-frequency waveform: the transmission starts at 2500 MHz and ends at 3500 MHz with steps in 1.5-MHz increments. The total active ("on") time of the stepped-frequency pulse is 1 μs. Between each active pulse is a 2-μs inactive ("off") period. A custom printed circuit board (PCB) is inserted between the RFSoC and the radar antennas to 1) lowpass filter and amplify the transmitted waveform and 2) highpass filter and amplify the received waveform. Two such PCBs are visible in Fig. 1b; both are powered from a single 28-VDC power supply.

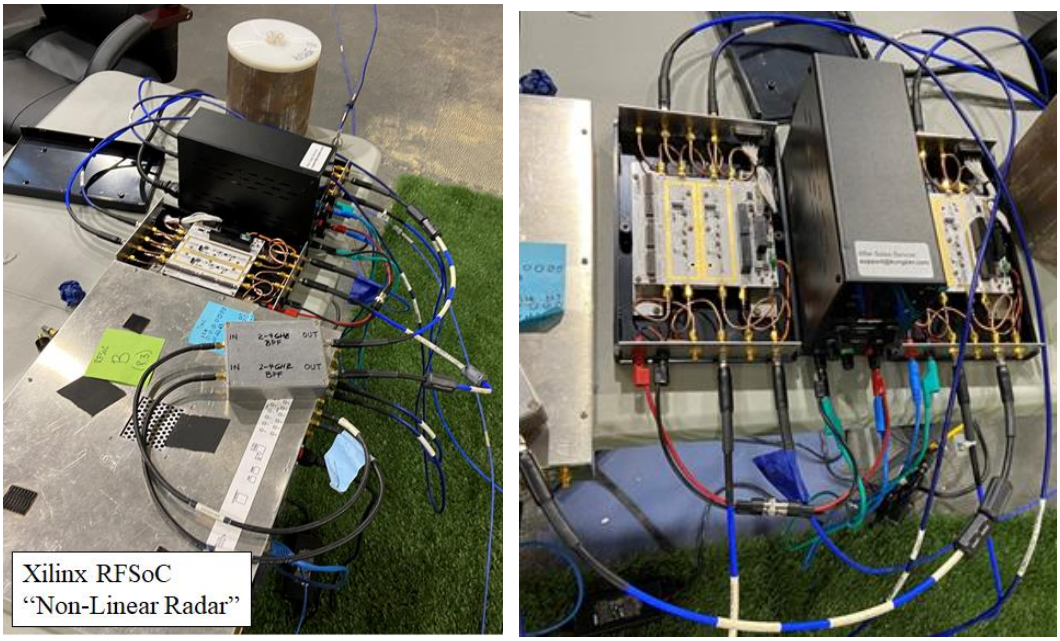

(a) (b)

Fig. 1 Stepped-frequency radar transceiver: (a) RFSoC by Xilinx with radar firmware by Alion/HII, and (b) custom transmitter/receiver (Tx/Rx) filter-and-amplifier PCBs powered by 28 VDC

A closer-up picture of one of the custom PCBs is shown in Fig. 2. The gain of the first transmitter (Tx_1), first receiver (Rx_1), second transmitter (Tx_2), and second receiver (Rx_2) are adjustable using the four sets of switches along the top of the PCB. In Fig. 1b Tx_1 and Rx_2 are routed through the left-most filter/amp set, while Tx_2 and Rx_1 are routed through the right-most filter/amp set. This arrangement minimizes near-field coupling between Tx_1 and Rx_1 and coupling between Tx_2 and Rx_2.

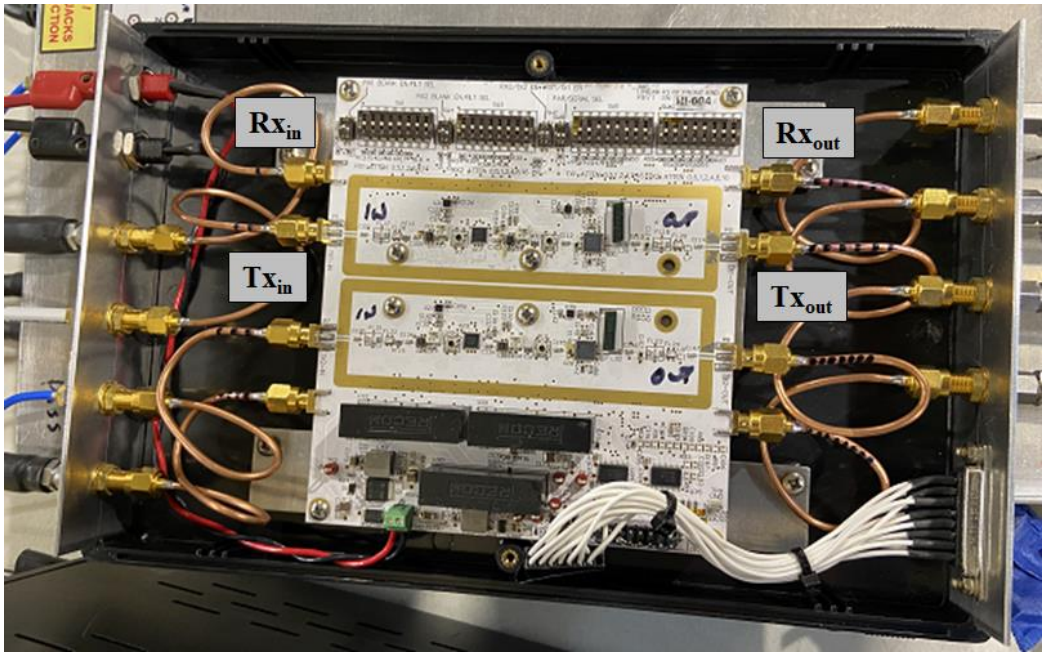

Fig. 2 This amplifier and filter PCB provides signal conditioning beyond the capabilities of the RFSoC to support nonlinear (harmonic) radar

The first pair of Tx/Rx antennas is located outside of "wall 1" along the plywood building, as seen in Fig. 3. The second pair of antennas is located outside of "wall 2," as seen in Fig. 4. The antenna pairs are orthogonal to each other; their Tx/Rx patterns intersect inside the plywood building in the center of the (unobstructed) test area.

Fig. 3 Experiment at ARL-ALC Building 507: Tx_1 and Rx_1 antennas pointed at the plywood building outside of "wall 1"

Fig. 4 Experiment at ARL-ALC Building 507: Tx_2 and Rx_2 antennas pointed at the plywood building outside of "wall 2" (door was closed during active data collections)

The inside of the plywood building is shown in Figs. 5 and 6. The camera view of Fig. 5 is looking back toward Tx_1/Rx_1 with Tx_2/Rx_2 on the right. The camera view of Fig. 6 is looking away from Tx_1/Rx_1 with Tx_2/Rx_2 on the left. For several data collections, the authors themselves acted as moving targets: "Dave" walked in front of "wall 1" (ahead of Tx_1/Rx_1), while "Greg" walked in front of "wall 2" (ahead of Tx_2/Rx_2).

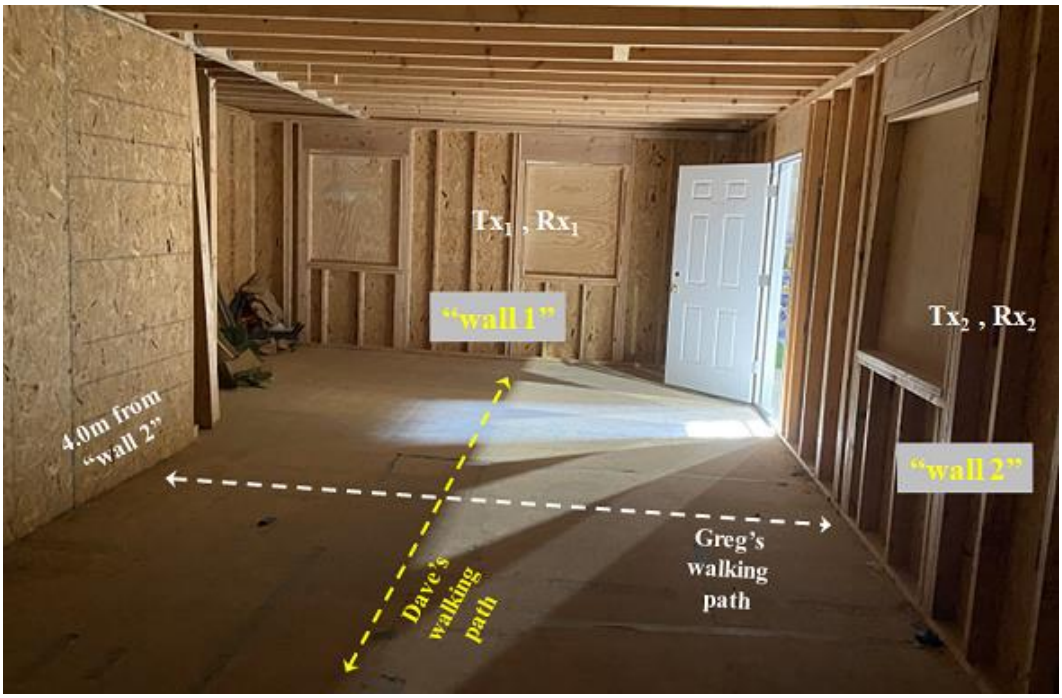

Fig. 5 Inside the plywood building: Dave's and Greg's walking paths, looking back toward the Tx/Rx antenna pairs

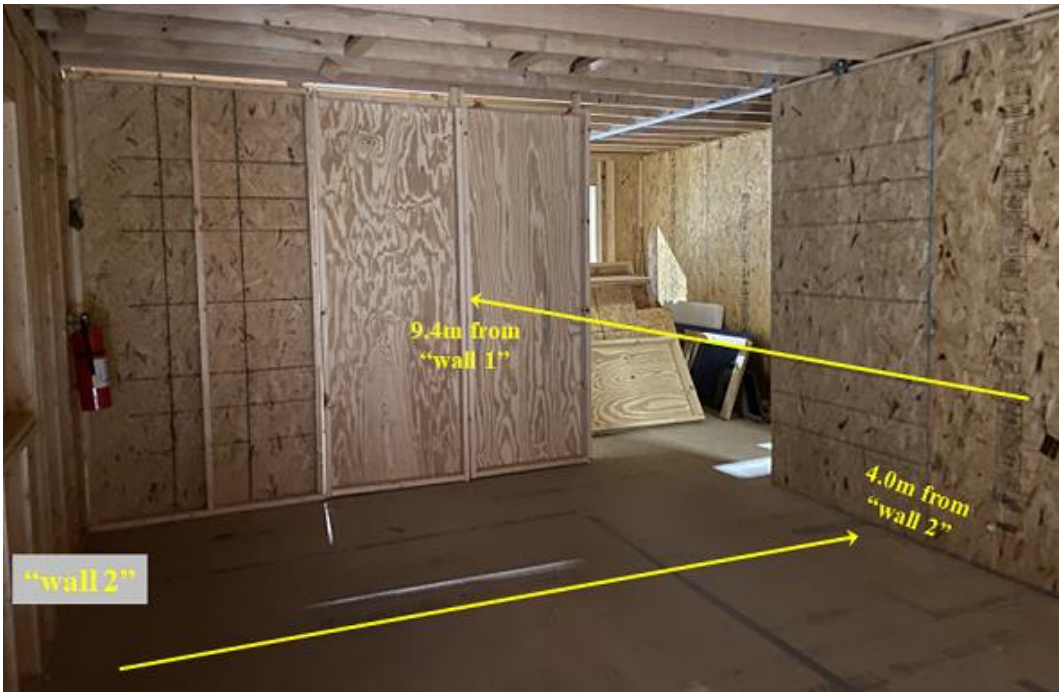

Fig. 6 Inside the plywood building: Dave's and Greg's walking paths, looking away from the Tx/Rx antenna pairs (fire extinguisher was removed while data was collected)

The RFSoC-based radar transmits and captures stepped-frequency pulses, appending a single file with two channels of received pulses, for as long as the user desires. Short data collections, when no targets were present or moving in the scene, lasted under 1 min. Longer data collections, when both authors walked back and forth inside of the building, lasted 7–8 min.

For the experiments reported here, the radar was always run in "linear" mode (i.e., the transmitted and received frequencies were identical). The radar captures data as in-phase and quadrature modulation on the instantaneous stepped carrier ("I/Q data"), and it computes an inverse fast Fourier transform (iFFT) to generate individual range profiles.

In Fig. 7 is a screenshot of HII's GUI. The radar displays (I/Q) amplitude-versus-time as pulses are sent and received; thus, raw data captured from both Rx channels is visible in real time. Figure 7 shows four consecutive frequency steps. Figure 8 is a screenshot of the iFFT computed from the complex amplitudes of the most recent complete set of received frequencies; thus, an amplitude-versus-range profile corresponding to the current scene is displayed in real time.

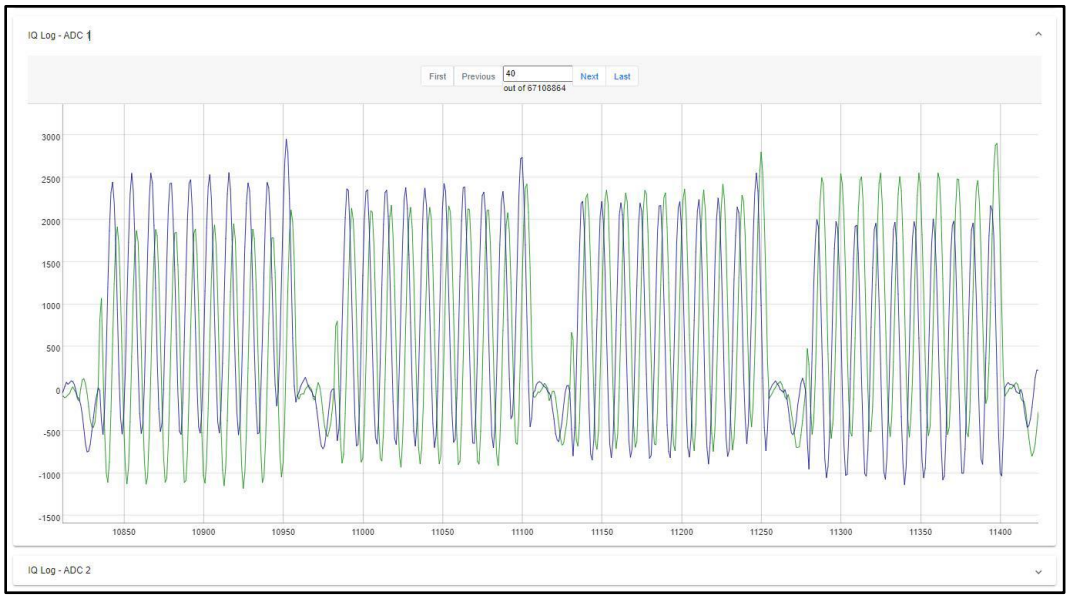

Fig. 7 HII's "Non-Linear Radar" GUI, showing a sequence of received stepped-frequency pulses as I/Q data (in-phrase = blue, quadrature = green)

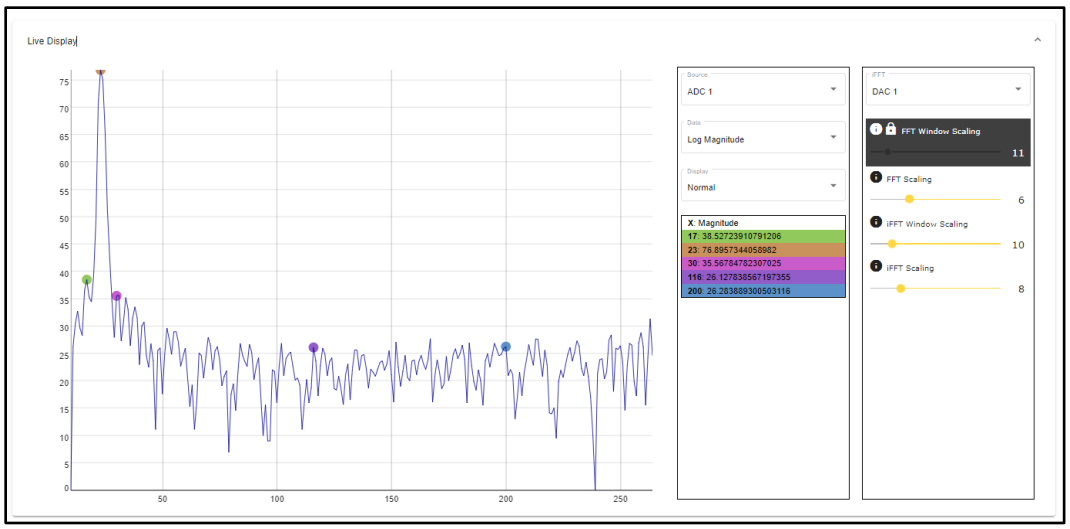

Fig. 8 HII's "Non-Linear Radar" GUI, processing received stepped-frequency pulses into a single amplitude-vs.-range profile

3. Data: Range Profiles Plotted Over Time

The aforementioned range profiles were regenerated in MATLAB from the raw I/Q data collected over time. Those profiles were re-oriented along the vertical axis, with lighter shades corresponding to larger amplitudes, and each collection—as a progression over time—was stacked along the horizontal axis. Figure 9 is a pair of such shaded colormaps, generated from the two simultaneous channels when the plywood building was empty.

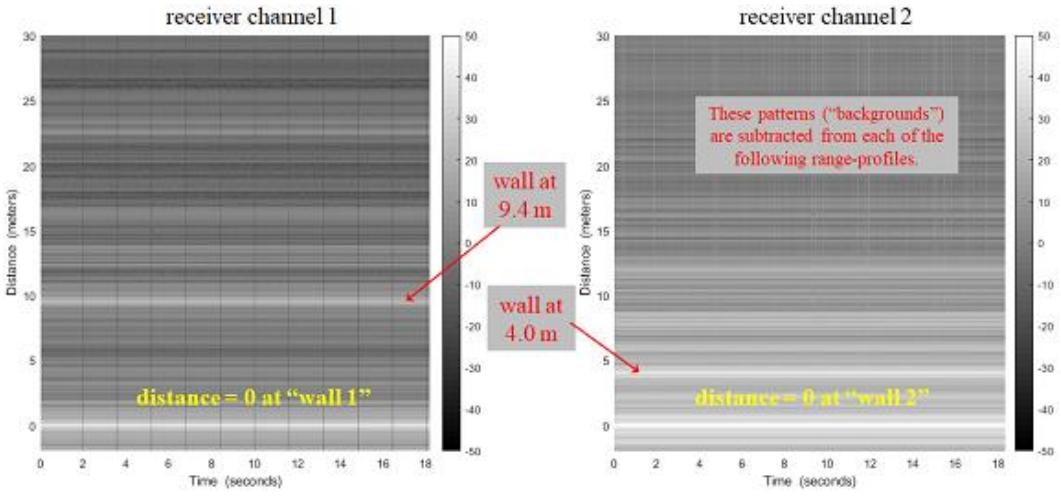

Fig. 9 Range profile images of the empty plywood building

Along each plot, the "distance" axis was rescaled such that "0 meters" corresponds to each outer wall ("wall 1" in front of Tx_1/Rx_1, and "wall 2" in front of Tx_2/Rx_2). In the Rx Channel 1 data, a bright line is visible at 0 m, and another bright line is visible at 9.4 m that represents the back wall of the test area across from "wall 1." In the Rx Channel 2 data, a bright line is visible at 0 m, and another bright line is visible at 4.0 m that represents the back wall of the test area across from "wall 2."

The first target placed in the building was a metal trihedral corner reflector sitting atop a 1-m-tall foam pedestal. The locations of the reflector/pedestal are drawn on Fig. 10, at two different distances away from "wall 1." The reflector and pedestal are shown in Fig. 11a.

Fig. 10 Inside the plywood building: locations of corner reflectors toward/away from antenna pair Tx_1/Rx_1

(a) (b) (c)

Fig. 11 (a) Trihedral corner reflector on foam pedestal, (b) tall metal sheet, and (c) laser distance-measurement tool

Range profiles collected when the reflector is stationary at 1.2 m beyond "wall 1" are given in Fig. 12. A bright line is clearly visible at the expected distance, in the Rx_1 data, in front of "wall 1." Range profiles collected when the reflector is located 9.3 m beyond "wall 1" are given in Fig. 13. Again, a bright line is clearly visible at the expected distance, in the Rx_1 data, in front of "wall 1."

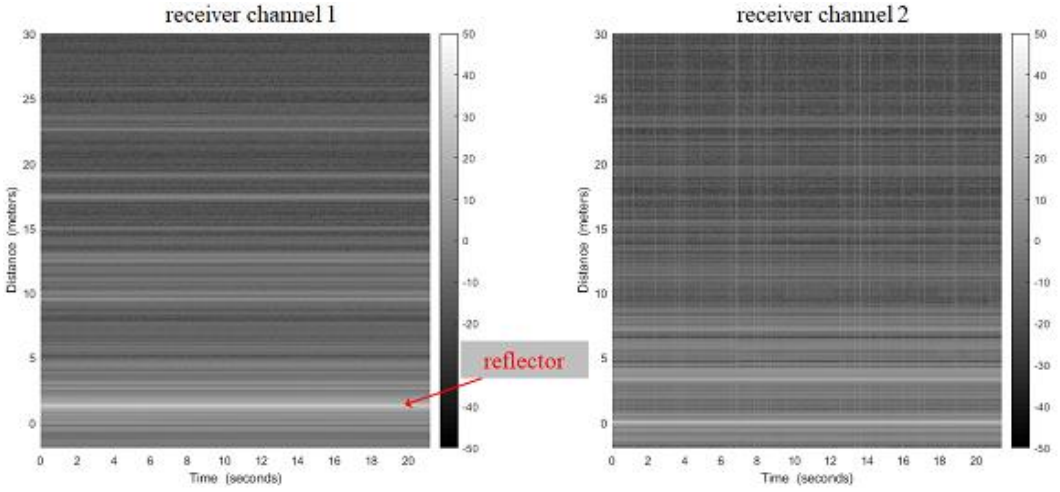

Fig. 12 Range profiles: corner reflector 1.2 m beyond "wall 1"

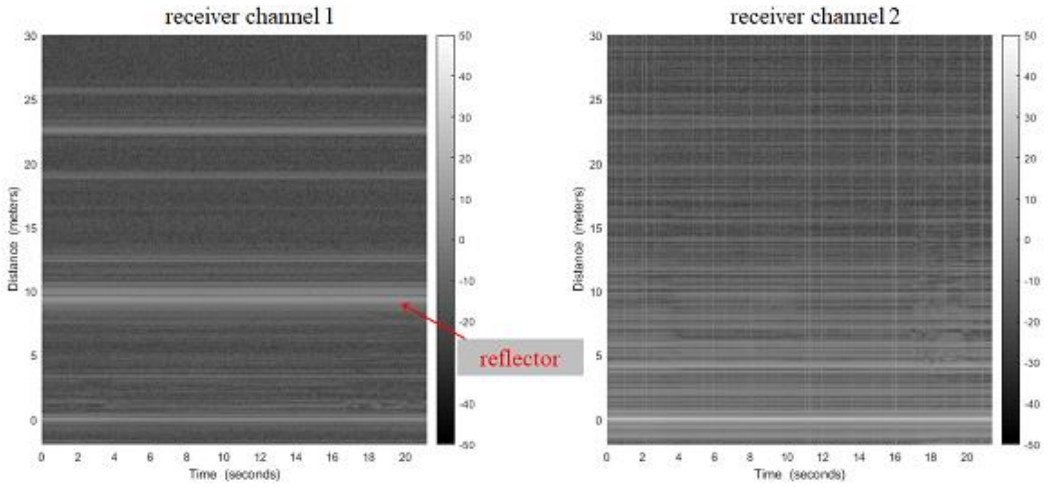

Fig. 13 Range profiles: corner reflector 9.3 m beyond "wall 1"

Next, author David McNamara ("Dave") walked back-and-forth between these two corner-reflector positions, steadily, for just over 90 s. In Fig. 14 a bright sawtooth waveform appears on Rx_1, which stretches between 0 and 9.3 m, corresponding to five-and-a-half "walks" toward and away from Tx_1/Rx_1. A periodic motion also appears on Rx_2, exactly twice the number of walks, which corresponds to 11 trips passing in front of Tx_2/Rx_2 (farther, closer, farther).

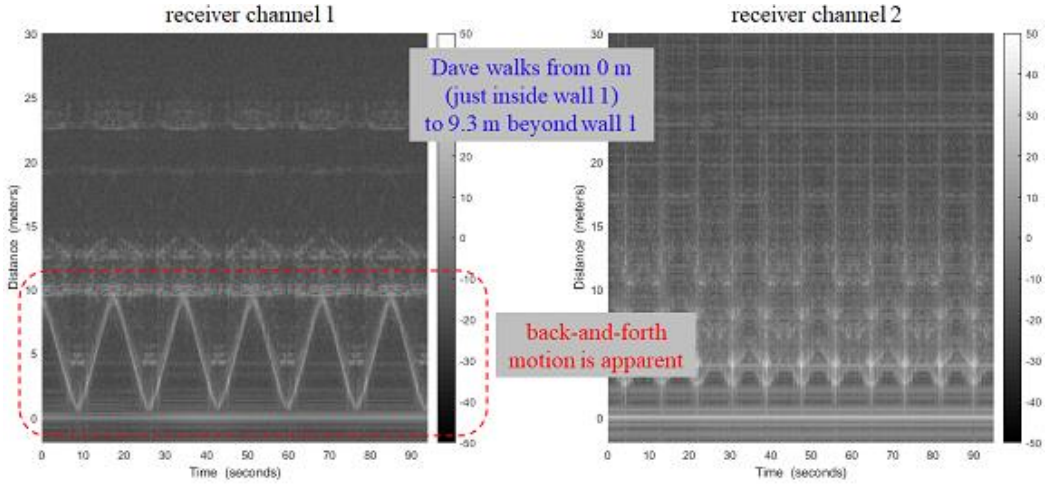

Fig. 14 Range profiles: Dave walking toward/away from antenna pair Tx_1/Rx_1

Two different locations of the reflector/pedestal are drawn on Fig. 15 at two different distances away from "wall 2." Range profiles collected when the reflector is at 1.3 m beyond "wall 2" are given in Fig. 16. A bright line is clearly visible at the expected distance, in the Rx_2 data, in front of "wall 2." Range profiles collected when the reflector is located 3.9 m beyond "wall 2" are given in Fig. 17. Again, a bright line is clearly visible at the expected distance, in the Rx_2 data, in front of "wall 2."

Fig. 15 Inside the plywood building: locations of corner reflectors toward/away from antenna pair Tx_2/Rx_2

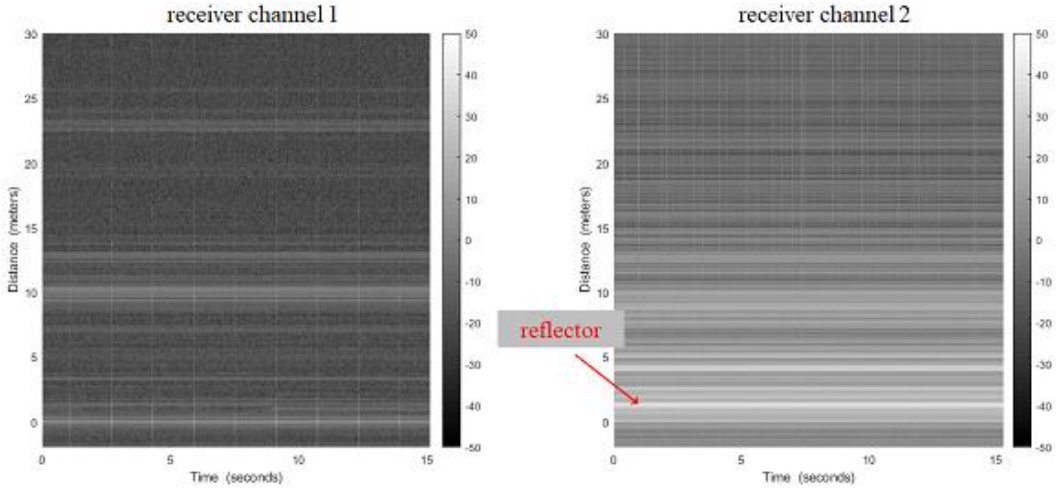

Fig. 16 Range profiles: corner reflector 1.3 m beyond "wall 2"

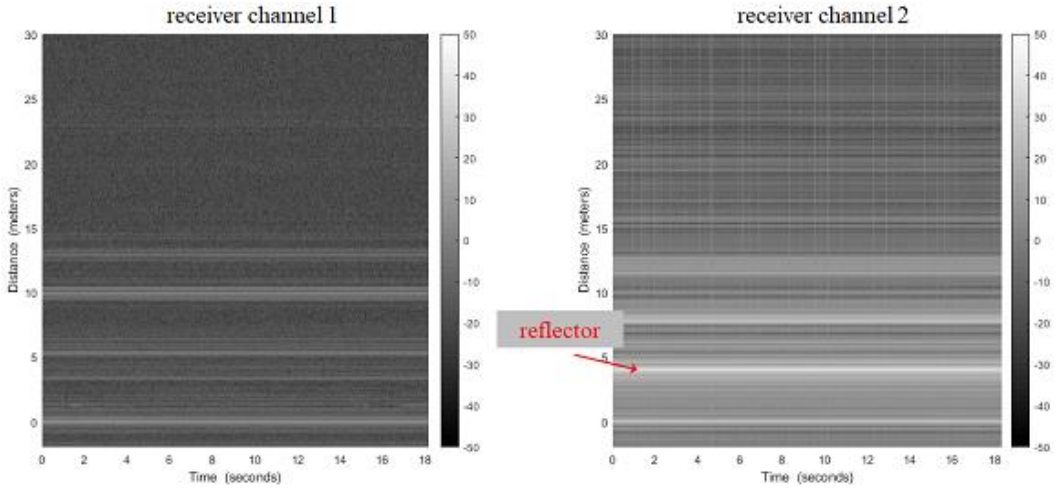

Fig. 17 Range profiles: corner reflector 3.9 m beyond "wall 2"

Author Gregory Mazzaro ("Greg") walked back and forth in front of Tx_2/Rx_2, steadily, for just under 90 s. In Fig. 18 a bright sawtooth waveform appears on Rx_2, which stretches between 0 and 3.9 m, corresponding to six walks toward and away from Tx_2/Rx_2. A periodic motion also appears on Rx_1, which corresponds to 12 trips passing in front of Tx_1/Rx_1. With both Dave and Greg walking, the range profiles of Fig. 19 were recorded. Dave's path is clearly resolvable from Rx_1, while Greg's path is resolvable from Rx_2.

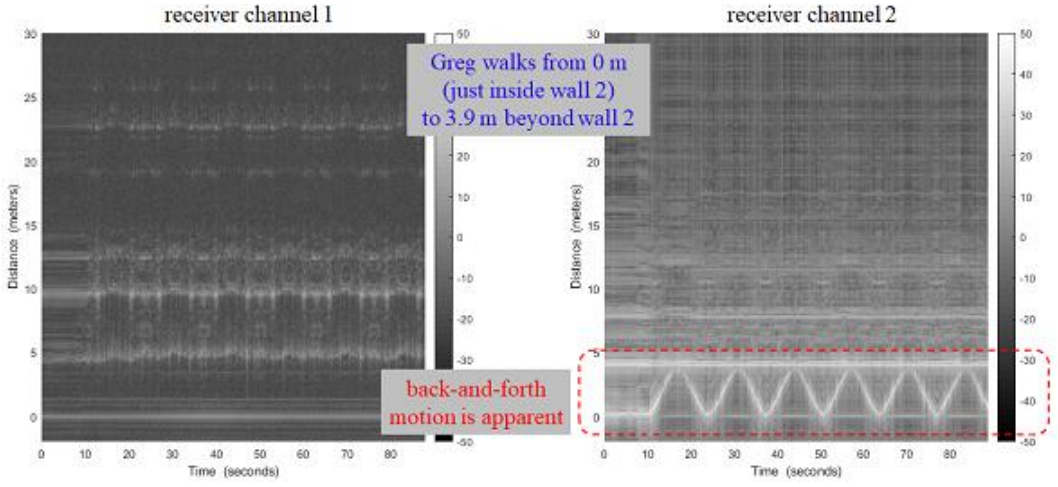

Fig. 18 Range profiles: Greg walking toward/away from antenna pair Tx_2/Rx_2

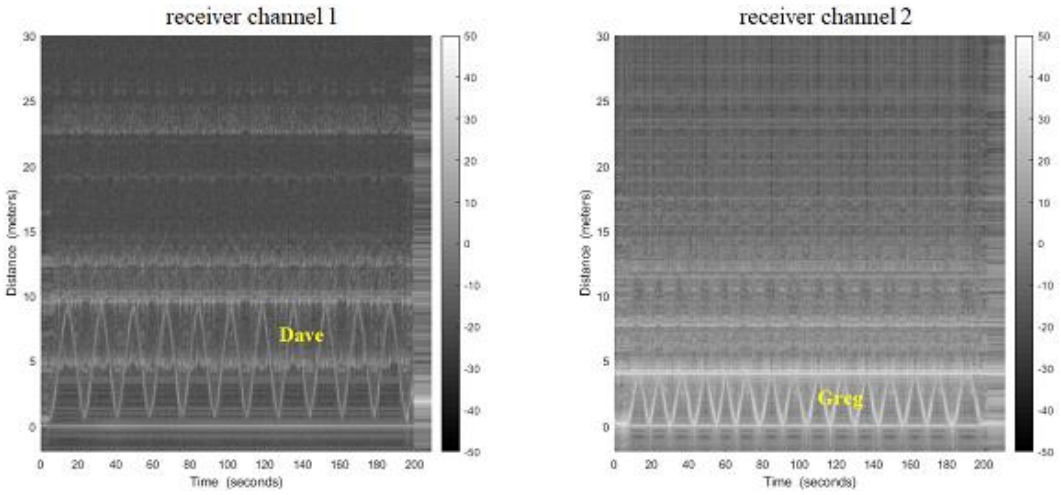

Fig. 19 Range profiles: Dave walking toward/away from antenna pair Tx_1/Rx_1 and Greg walking toward/away from antenna pair Tx_2/Rx_2

4. Creation of False Alarms that Track Real Targets

To generate additional "ghost" images of moving targets (with the intention of removing those "ghosts" from the Rx_1 range profiles using data collected from Rx_2, and vice versa), metal sheets (approximately 2 m tall) were placed in-line with the antenna pairs, directly across from "wall 1" and "wall 2" (Fig. 20). A picture of one of the metal sheets is provided in Fig. 11b.

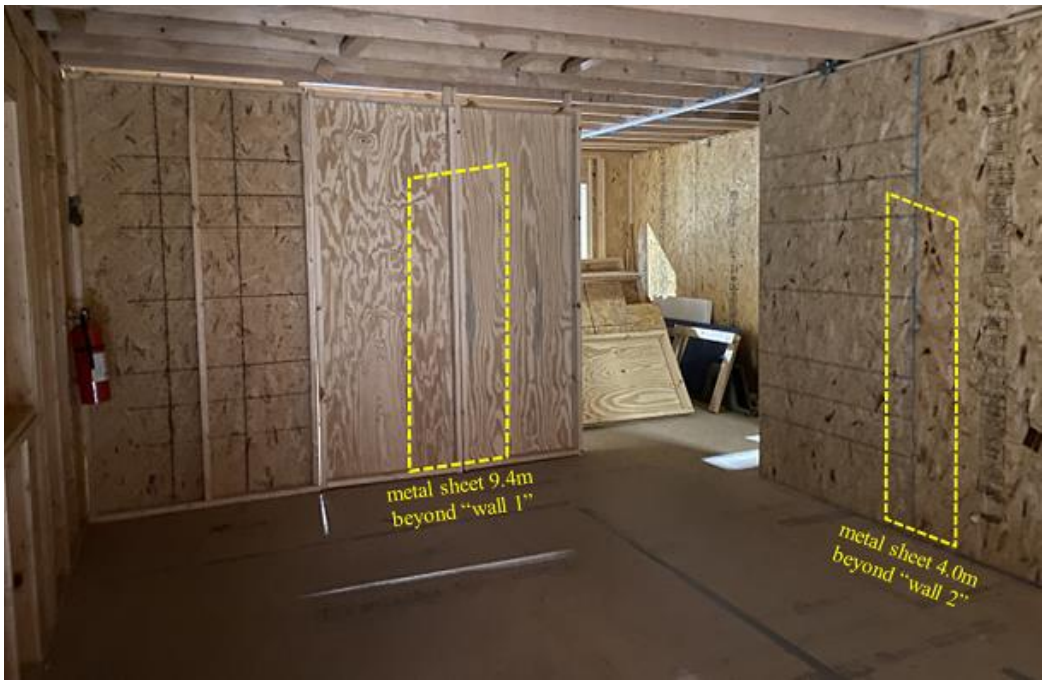

Fig. 20 Inside the plywood building: locations of metal sheets

By imaging the static empty-test-area case in Fig. 21, the metal sheets are observed as wider, brighter lines along where "wall 1" and "wall 2" are located (as compared to the thinner, darker lines of Fig. 9).

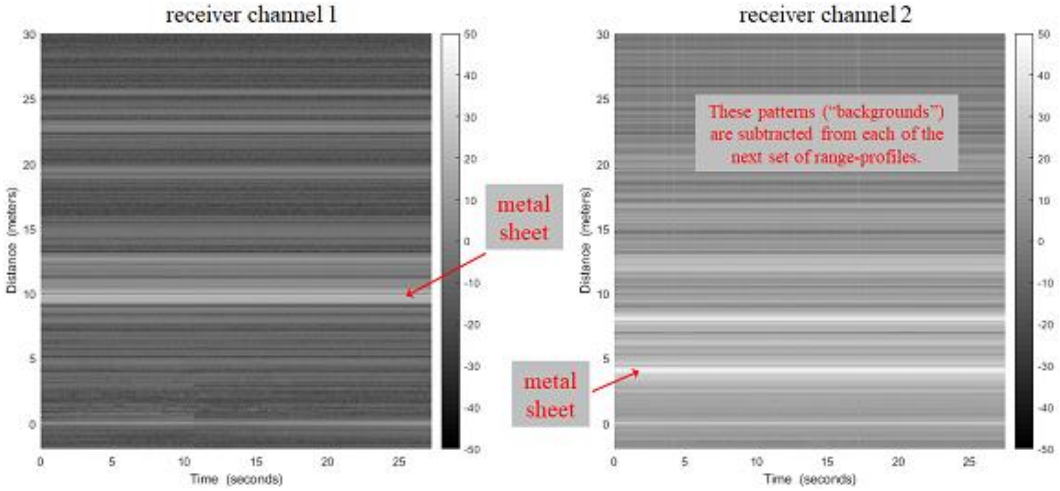

Fig. 21 Range profiles: metal sheets placed 9.4 m beyond "wall 1" and 4.0 m beyond "wall 2"

The data of Figs. 14, 18, and 19 was recaptured as Figs. 22–24, now with the two metal sheets along the two inner/back walls. In Figs. 22 and 23, both Dave and Greg were present in the scene: while one walked, the other remained stationary just behind "wall 1" or "wall 2."

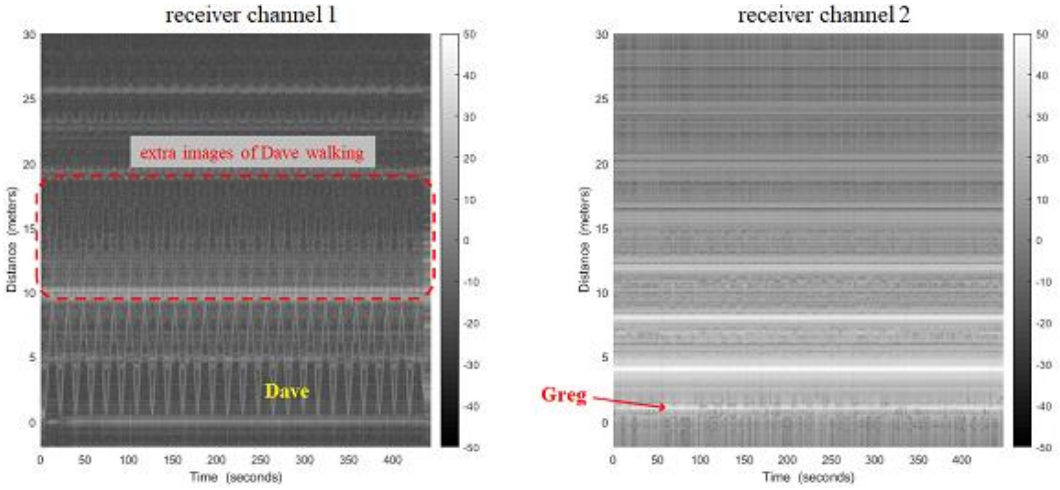

Fig. 22 Range profiles: Dave walking toward/away from antenna pair Tx_1/Rx_1 and Greg standing 1.3 m beyond "wall 2"; metal sheets present

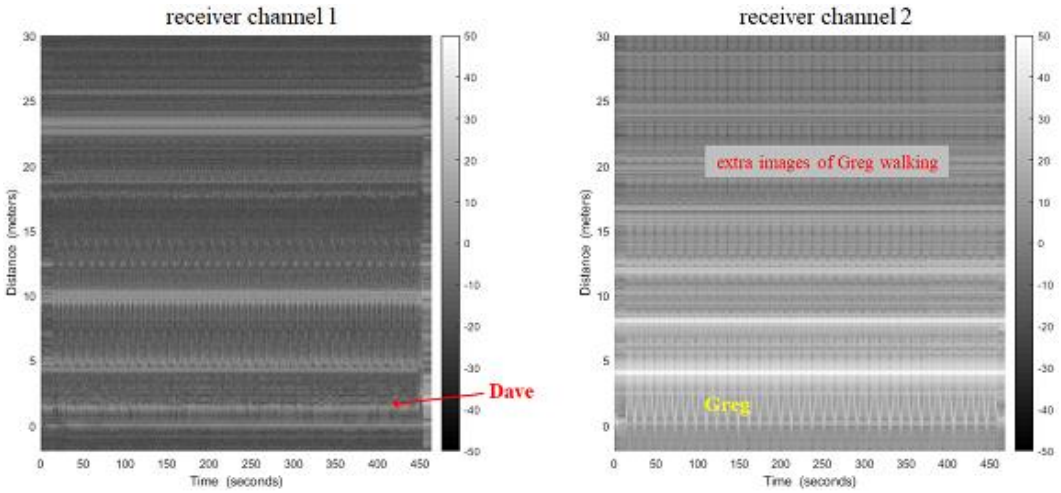

Fig. 23 Range profiles: Dave standing 1.2 m beyond "wall 1" and Greg walking toward/away from antenna pair Tx_2/Rx_2; metal sheets present

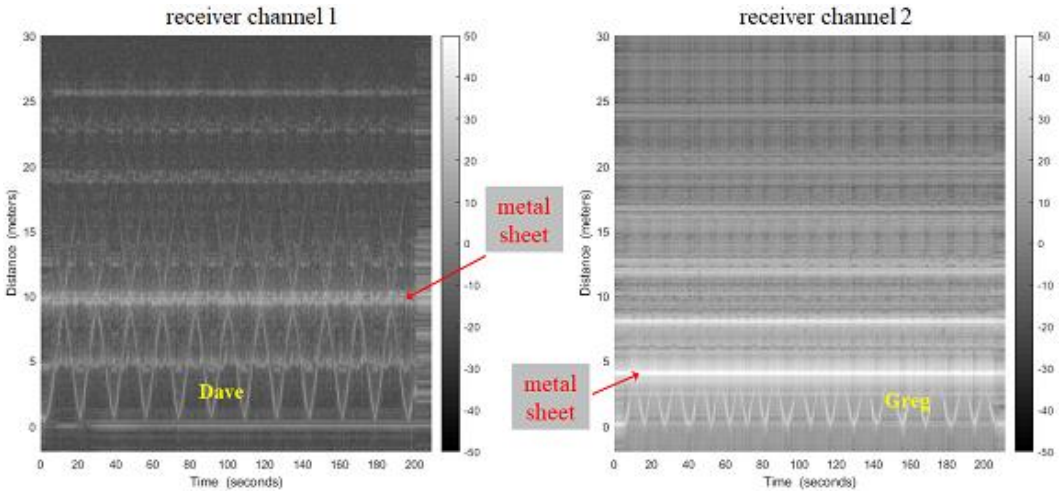

Fig. 24 Range profiles: Dave walking toward/away from Tx_1/Rx_1 and Greg walking toward/away from Tx_2/Rx_2; metal sheets present

In Figs. 22 and 23, "ghost" images appear behind the true targets. In Rx_1 in Fig. 22, a second sawtooth waveform appears between 10 and 18 m away from "wall 1," and a third periodic waveform is faint but visible beyond 20 m. In Rx_2 (Fig. 23), periodic waveforms fill nearly the entire imaged space beyond the wall at 4.0 m. In Fig. 24, both Dave and Greg are discernible as targets moving in front of their respective receivers.

5. Bistatic Distributed Radar

A bistatic variation of the previous experiment was also conducted. The coaxial connections to the two transmitter antennas were swapped: Tx_1 (previously paired with Rx_1) was paired with Rx_2, and Tx_2 (previously paired with Rx_2) was paired with Rx_1, as noted in Fig. 25. The empty test area was imaged as shown in Fig. 26.

Fig. 25 Experiment at ARL-ALC Building 507: Tx antenna connections swapped to simulate a bistatic radar

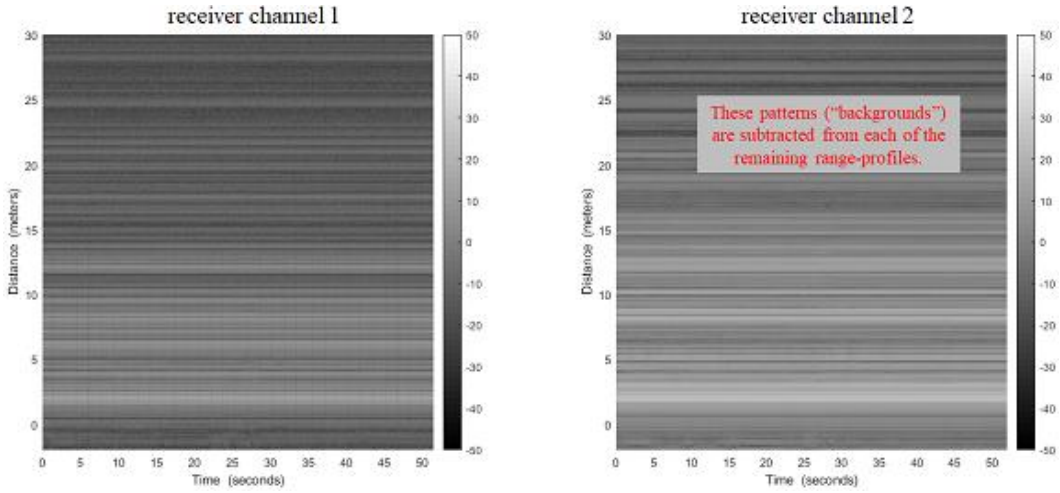

Fig. 26 Range profiles: bistatic radar, two metal sheets (9.4 m beyond "wall 1" and 4.0 m beyond "wall 2")

The data of Figs. 22–24 was recaptured and regenerated for the bistatic case as Figs. 27–29. Periodic motion is observed on both channels in Fig. 27 when only Dave is walking, and periodic motion is observed on both channels in Fig. 28 when only Greg is walking. In Fig. 29, with two people moving in the scene, visual identification and separation of the two walking paths are not possible; it appears

that range-Doppler processing or a more sophisticated algorithm is required to discern the two targets.

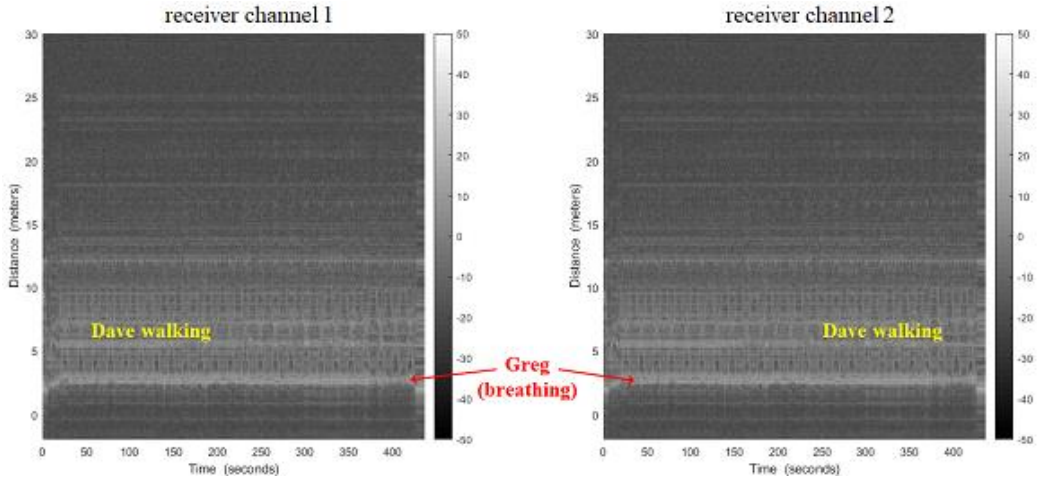

Fig. 27 Range profiles, bistatic radar: Dave walking toward/away from Tx_2/Rx_1 and Greg standing 1.3 m beyond "wall 2"

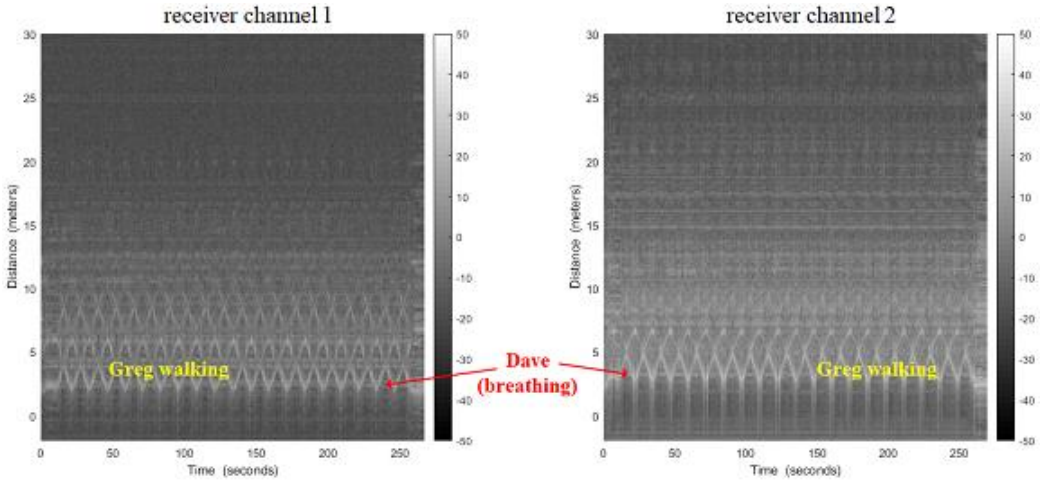

Fig. 28 Range profiles, bistatic radar: Dave standing 1.2 m beyond "wall 1" and Greg walking toward/away from Tx_1/Rx_2

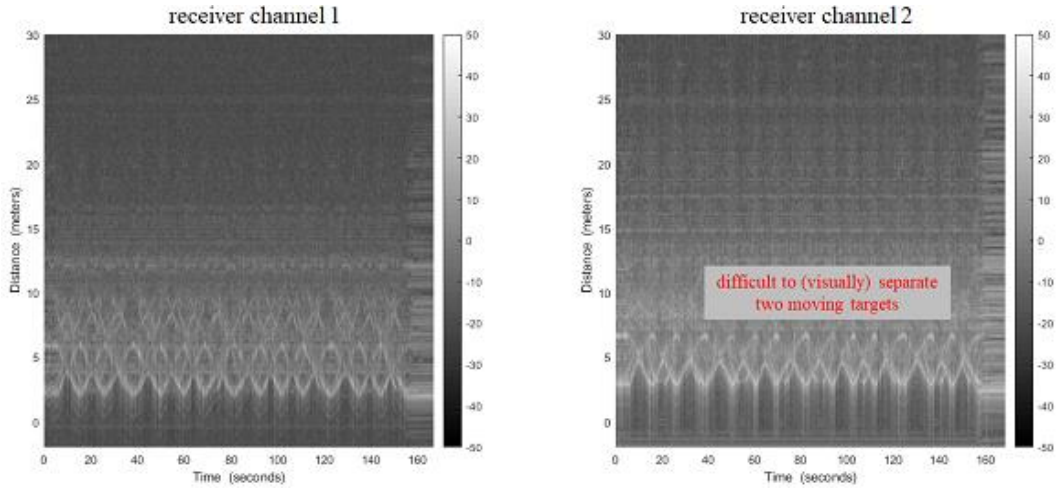

Fig. 29 Range profiles, bistatic radar: Dave walking to/from Tx_2/Rx_1 and Greg walking to/from Tx_1/Rx_2

6. Conclusion and Follow-On Work

The data collected in this study indicates that antenna pairs looking into a low-metal building and at right angles to each other are able to detect multiple moving targets when those targets are otherwise not visible from outside the building. Mapping distance over time reveals the path that a target follows; ambiguity regarding a target's path tracked in one channel may be mitigated by tracking the same target on another channel. Work remains to coherently combine the IQ amplitudes from the simultaneous data collections to resolve multiple targets. One goal is to map target locations on a 2-D (down-range and cross-range) image, presented perhaps as a video animation overlaid on an overhead view of the scene (i.e., a typical floorplan for the building being imaged). It remains to be determined whether a bistatic pairing of transmitter and receiver antennas provides an advantage (over the standard mono-static transmitter-antenna pairing) when imaging moving targets.

7. References

1. Martone A, Ranney K, Innocenti R. Through-the-wall detection of slow-moving personnel. Proceedings of SPIE. Apr 2009;7308:73080Q(1–12).

2. Martone A, Ranney K, Innocenti R. Automatic through the wall detection of moving targets using low-frequency ultra-wideband radar. Presented at the 9th IEEE International Radar Conference; 2010 May.

3. Phelan BR, Ressler MA, Ranney KI, Smith GD, Kirose GA, Sherbondy KD, Narayanan RM. Performance analysis of spectrally versatile forward-looking ground-penetrating radar for detection of concealed targets. Proceedings of SPIE. 2015 May;9461:94610J(1–10).

4. Phelan BR, Ranney KI, Gallagher KA, Clark JT, Sherbondy KD, Narayanan RM. Design of ultrawideband stepped-frequency radar for imaging of obscured targets. IEEE Sensors. May 2017;17(14):4435–4446.

5. Mazzaro G, Gallagher K, Sherbondy K, Salik K. Through-the-wall detection of nonlinear junctions. DEVCOM Army Research Laboratory (US): 2021 June. Report No.: ARL-TR-9229.

6. Mazzaro GJ, Martone AF, Ranney KI, Narayanan RM. Nonlinear radar for finding RF electronics: System design and recent advancements. IEEE Trans Microw Theory Techn. 2017 May;65(5):1716–1726.

List of Symbols, Abbreviations, and Acronyms

2-D	two-dimensional
ALC	Adelphi Laboratory Center
ARL	Army Research Laboratory
DC	direct current
DEVCOM	US Army Combat Capabilities Development Command
GUI	graphical user interface
HII	Huntington Ingalls Industries
iFFT	inverse fast Fourier transform
I/Q	in-phase and quadrature modulation
PCB	printed circuit board
Rx_1	first receiver
Rx_2	second receiver
RFSoC	radio-frequency system-on-a-chip
Tx_1	first transmitter
Tx_2	second transmitter
VDC	volts direct current

1 DEFENSE TECHNICAL
(PDF) INFORMATION CTR
DTIC OCA

1 DEVCOM ARL
(PDF) FCDD RLB CI
TECH LIB

5 DEVCOM ARL
(PDF) FCDD RLA LC
A BOUVY
K GALLAGHER
G MAZZARO
D MCNAMARA
K SHERBONDY